

Self-assembled polyelectrolyte nanorings observed by liquid-cell AFM

This article has been downloaded from IOPscience. Please scroll down to see the full text article.

2004 J. Phys.: Condens. Matter 16 S2109

(<http://iopscience.iop.org/0953-8984/16/22/009>)

View [the table of contents for this issue](#), or go to the [journal homepage](#) for more

Download details:

IP Address: 129.252.86.83

The article was downloaded on 27/05/2010 at 14:59

Please note that [terms and conditions apply](#).

Self-assembled polyelectrolyte nanorings observed by liquid-cell AFM

J-Luis Menchaca¹, Héctor Flores^{2,3}, Frédéric Cuisinier³ and Elías Pérez¹

¹ Instituto de Física, Universidad Autónoma de San Luis Potosí, Alvaro Obregón 64, San Luis Potosí, Mexico

² Facultad de Estomatología, Universidad Autónoma de San Luis Potosí, Alvaro Obregón 64, San Luis Potosí, Mexico

³ INSERM U 595, Federation de Recherche Odontologiques, Université Louis Pasteur, 11 rue Humann, 67085 Strasbourg Cedex, France

Received 11 October 2003

Published 21 May 2004

Online at stacks.iop.org/JPhysCM/16/S2109

DOI: 10.1088/0953-8984/16/22/009

Abstract

Self-assembled polyelectrolyte nanorings formed by polyelectrolytes are presented for the first time in this work. They are formed by poly(ethylenimine) (PEI) and poly(sodium 4-styrenesulfonate) (PSS) during the two first steps of the formation of the self-assembled polyelectrolyte films (SAPFs). These are formed on a negatively charged glass surface and observed by an *in situ* liquid-cell AFM technique, which has recently been introduced as an alternative technique to follow polyelectrolyte multilayer formation without drying effects (Menchaca *et al* 2003 *Colloids Surf. A* **222** 185). Nanoring formation strongly depends on the preparation method and parameters such as polyelectrolyte filtration, air and CO₂ presence during SAPFs formation and buffer solution. A necessary condition to obtain nanorings is that polyelectrolyte solutions have to be filtered prior to injection into the liquid-cell AFM. The outer diameter of nanorings can be varied from hundreds of nanometres to microns by changing these parameters. Nanorings are stable in the liquid cell for hours but they disappear on contact with air. Additionally, carbonate ions seem to be mainly responsible for the formation of this novel structure.

(Some figures in this article are in colour only in the electronic version)

1. Introduction

Self-assembled polyelectrolyte films (SAPFs), formed by sequential adsorption of polycations and polyanions in aqueous solution on a charged surface, have been introduced as a new method to modify surfaces [2]. In order to study their surface structure, we have recently

introduced a liquid-cell AFM technique, which allows us to follow the multilayer build-up in an *in situ* set-up. In this methodology, external effects are minimized or eliminated during the polyelectrolyte assembling; for instance, drying effects are completely eliminated. This technique has shown that the surface of polyelectrolyte films have a lateral structure; SAPFs form granular domains on their surface that are formed by complexes of positive and negative polyelectrolytes [1]. This technique reveals the SAPF surface as a complex system: it has also shown that grain size, number and surface roughness change with time following its own kinetics and the polyelectrolyte surface structure strongly depends on the preparation method [1]. These results can only promote theoretical and computational work. For instance, granulate structure has already been reproduced by Monte Carlo simulations [3]. However, lateral structure has not yet been considered in theoretical models of SAPFs [4, 5].

In this paper, we report a novel ring polyelectrolyte structure formed by two polyelectrolytes on a negatively charged glass surface at the beginning of SAPFs formation. We call this structure a nanoring because, independent of the lateral ring dimensions, the height is only a few nanometres.

It is possible that the mechanisms that produce these nanorings are related to those that produce DNA condensation, giving toroidal structures. DNA in aqueous solution is a highly negative charged polymer with a long persistent length [6]. DNA condensation refers to DNA aggregates with finite size and some morphology produced by different precipitants: multivalent ions alcohols, basic proteins, neutral polymers and cationic liposomes [7]. In order to explain DNA condensation, it has been recognized that two like-charged polyelectrolyte attractions are mediated by their counterions [9]. The fluctuation and correlation of these counterions explain the attraction between like-charged polyelectrolytes [8]. In addition, integral equation theory and Monte Carlo simulation have shown the importance of the ion and counterion size and valence to explain the attraction between like-charged macro-ions and a wall [10].

It has also been recognized that DNA internal structure plays an important role in this toroidal condensation [11]. This dependence is also clearly shown in the self-assembling peptide nanorings and nanotubes, where D- and L-amino acid residues form these structures by steric constraints and noncovalent bonds [12, 13].

It is worth mentioning that DNA condensation and like-charged polyelectrolyte attraction is only observed in the presence of multivalent ions in solution. For polyelectrolyte nanorings presented here, divalent ions are provided by the carbonate ions from air, directly introduced by cleaning with CO₂ or using a carbonate buffer. In this first work, we determined some parameters influencing nanoring formation. They are mainly related to the preparation method: polyelectrolyte filtration, air and CO₂ presence during SAPFs formation and buffer solution.

2. Materials and methods

Materials and buffer preparation

Poly(ethylenimine) (PEI), poly(sodium 4-styrenesulfanate) (PSS) and poly(allylamine hydrochloride) (PAH) ($M_w \approx 70\,000$ Da, Sigma) solutions were prepared in carbonate and TRIS–MES buffers at 1 mg ml^{-1} . Carbonate buffer is prepared with 15 mM of sodium carbonate (Na₂CO₃) and 35 mM of acid sodium carbonate (NaHCO₃). MES–TRIS buffer contains 25 mM of tris(hydroxymethyl) aminomethane (TRIS) and 2-(*N*-morpholino) ethanesulfonic (MES) with 100 mM of NaCl (Sigma, USA). In both cases pH was adjusted with HCl and NaOH solutions at 0.1 M. MES–TRIS buffer was used at pH = 6.8 and carbonate buffer at pH = 8.5, 9.0 and 9.5. All solutions were prepared with ultrapure water (Mill Q-Plus

system, Millipore) with a resistivity of $18.2 \text{ M}\Omega \text{ cm}$. The polyelectrolyte solutions and buffer were filtered (Millex PVDF, Millipore, USA and PTFE, Nalgene, USA) with filters of 0.10, 0.22 and $0.45 \mu\text{m}$ pore size. Carbonate buffer was used to control the presence of (CO_3^{2-}) in the solution. Carbon dioxide (CO_2) is naturally adsorbed from air in water and it produces two negative carbonate ions: a monovalent (HCO_3^-) and a divalent (CO_3^{2-}) ion. The concentration of carbonate ions depends on the pH values of the carbonate buffer. The presence of divalent carbonate ions is ensured by pH values higher than 8.0 [14].

Liquid-cell AFM

Observations were made with an AFM nanoscope IIIa of Digital Instruments (Santa Barbara, CA, USA), cantilevers with a spring constant of 0.01 N m^{-1} and silicon nitride tips were used (MLCT-AUHW, Park Scientific, USA). Tips were previously silanized with octadecyltrichlorosilane (OTS, 95%, Aldrich, USA) to turn hydrophilic tips into hydrophobic ones. Height and friction images were captured simultaneously in contact mode, but only the height images are reported here because they have equivalent information. Images were taken at 1 Hz scan rate with a resolution of 512×512 pixels. The scanning area sizes were 20, 10, 5 and $2.5 \mu\text{m}$.

SAPFs preparation

Glass slides of 14 mm in diameter (Micro Cover Glass, France) are first cleaned. They are cleaned in Helmanex solution at 3%, then heated at 60°C for 15 min. After rinsing, they are heated in 1% H_2SO_4 solution for 15 min at 60°C and finally dried with nitrogen (Air-Liquide, France) or cleaned with CO_2 gas (Air-Liquide, France) or CO_2 snow jet cleaning (Applied Surface Technologies, USA). The glass slides are mounted on an AFM piezoelectric. The cell is closed with a silicone o-ring. The aqueous solution (buffer) is injected into the cell and an image of the glass surface is taken for testing the AFM liquid cell. The positive polyelectrolyte PEI solution is then injected and left for 15 min in contact with the glass, a rinsing with 5 ml of aqueous solution is done and then the PEI surface is imaged. Similar steps are followed by the negative PSS and after by the positive PAH polyelectrolytes. MES-TRIS buffer, at $\text{pH} = 6.8$, was used in all the preparations, except for high pH values where carbonate buffer was used.

3. Results and discussion

A negative glass surface is used as the substrate for the SAPFs in this work. The typical roughness observed on this surface is less than 1 nm and corresponds to a negatively charged surface. SAPFs build-up is then started by the adsorption of a positive polyelectrolyte, using the procedure explained above. PEI adsorbed on the glass surface is shown in figure 1. A rough surface is observed, which reflects only the imperfections on the glass surface. Following SAPFs formation, PSS is then injected and rinsed. Polyelectrolyte film formed after this process is shown in figure 2. We observed a circular structure and the shape is closely related to rings on the images. They are uniformly distributed and ring sizes are relatively uniform for each experiment; outer diameters for the rings in figures 2(A) and (B) are 2780 ± 490 and 605 ± 70 nm, respectively, corresponding to a dispersion of 18% and 12%, while heights are 5.87 ± 3.9 and 3.44 ± 0.68 nm for figures 2(A) and (B), respectively. The different sizes were produced by changing the preparation step between PEI and PSS injection. Nanorings shown in figure 2(A) were obtained by the presence of air between the PEI and PSS deposition, while these shown in figure 2(B) were produced taking two hours between each polyelectrolyte



Figure 1. AFM image of PEI adsorbed on the glass surface. A PEI film does not produce nanoring structures (image: $5 \times 5 \mu\text{m}$; z range: 5 nm).

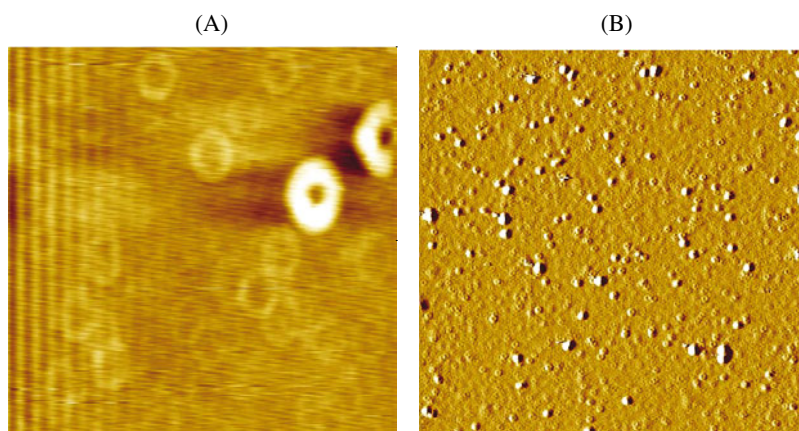


Figure 2. Nanorings formed by PEI-PSS polyelectrolyte in MES-TRIS buffer are produced when (A) air is introduced between PEI and PSS injection and (B) a long time (2 h) is taken between PEI and PSS injections. The sizes obtained were: 2780 ± 490 nm and 605 ± 70 nm, respectively (images: $20 \times 20 \mu\text{m}$; z range: 30 nm).

injection. A schematic representation of the polyelectrolyte nanorings is shown in figure 3, where the height (h) and the outer (D) and inner (d) diameters are defined. The nanoring structure has an outer diameter ranging from hundreds of nanometres to microns but the height is always of a few nanometres, independent of its diameter. This is the reason we call them nanorings.

The nanorings presented here were only observed after adsorption of PSS on PEI. The PEI surface was checked systematically in the experiments and we never observed a noticeable structure on the PEI film (see figure 1). This suggests that nanorings are formed by complexes of negative (PSS) and positive (PEI) polyelectrolytes.

In order to test this hypothesis, we carried out a second experiment injecting into the AFM cell a solution made by mixing PEI and PSS solutions at equal concentrations (1 mg ml^{-1})

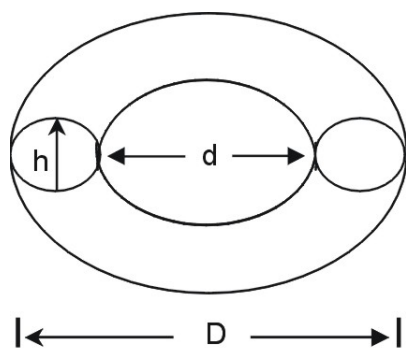


Figure 3. Schematic representation of the polyelectrolyte rings. D and d define the outer and inner diameters of the nanorings, h represents the height.

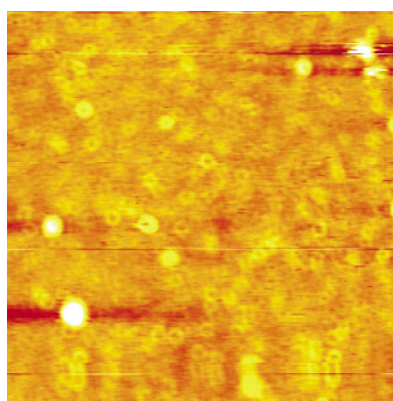


Figure 4. Ring structures obtained when polyelectrolyte PSS–PEI complexes are formed prior to injection. Complex and ring formation strongly depend on air contained in the preparation tubes (image: $20 \times 20 \mu\text{m}$; z range: 30 nm).

prepared previously. We observed nanorings with their characteristic shape, as is shown in figure 4. D in this case is of 990 ± 70 nm, an intermediate size between results the nanorings presented in figure 2. This proves that nanorings are formed by polyelectrolyte complexes. However, it is very difficult to establish if nanorings are already formed in solution, because of limitations of the AFM technique. We can only observe polyelectrolytes on the surface. An alternative method can be used to study polyelectrolyte micelles in solution where the formation of nanorings also seems possible [21].

The formation of nanorings in the experiments presented here strongly depends on time of contact with air during the experiment. When the solution is stored out of contact with air with fresh water produced by the Millipore system, it is impossible to produce nanorings. The biggest nanorings observed in our experiment are shown in figure 2(A) and were obtained after bubbling air between PEI and PSS injection. During the formation of nanorings by PEI–PSS complex injection, the presence of air was also important. PEI–PSS complexes were prepared in tubes of 10 ml with different air–solution proportions. Depending on the air–solution proportion, after a given time, polyelectrolyte solutions are more turbid for high air content. Air presence is a parameter to control polyelectrolyte complexes and consequently the nanorings.

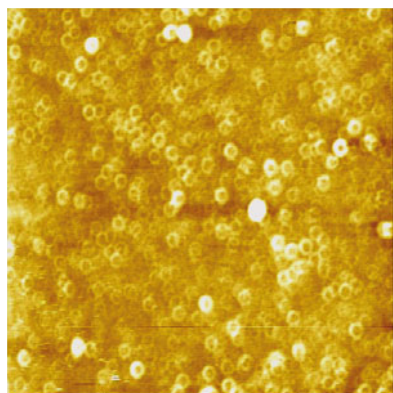


Figure 5. Polyelectrolyte rings formed by PEI–PSS polyelectrolytes on a glass surface previously cleaned with a CO₂ snow jet. PSS was injected after PEI (image: 10 × 10 μm; z range: 10 nm).

Taking as reference the main role that multivalent ions play in the DNA condensation and the attraction between like charged macro-ions, we assume that air presence is important for the divalent carbonate ions that are formed when carbon dioxide, from air, is dissolved in water. The quantity of CO₂ is directly related to the time and quantity of air in contact with polyelectrolyte solutions. The dissolution of CO₂ into water is then a possible mechanism that controls the formation of nanorings. With the purpose of introducing additional CO₂ into the experiments, we cleaned the glass surface with a CO₂ snow jet just before closing the liquid cell. Nanorings were again obtained with clear definition, as shown in figure 5, where we can observe the homogeneous nanoring distribution on the image. The outer diameter for this case was 204 ± 12 nm, giving a dispersion of 6%, the lowest obtained in our experiments.

Experiments in the presence of divalent carbonate ions (CO₃²⁻) from a carbonate buffer were then carried out. The presence of divalent ions is ensured for pH values higher than 8.0 [14]. However, the pH window is limited because PEI losses charge at higher pH: the pK of PEI is around 10.5. Three buffers were prepared at pH 8.5, 9.0 and 9.5. Nanorings were successfully obtained at pH 8.5 and 9.0 and shown in figure 6, respectively. At pH 9.5 we did not observed nanorings. This is certainly due to the charge loss of PEI because the pH is close to its pK. Nanoring size also depends on pH. At pH 8.5 the size is 303 ± 30 nm and at pH 9.0 1240 ± 96 nm. The size is greater at high pH value, where the presence of divalent carbonate ions is higher.

We have observed that these nanorings were destroyed when the liquid cell is empty and therefore when polyelectrolyte films are partially dried. We have only observed nanorings when the liquid-cell AFM contains an aqueous solution. SAPFs have been previously imaged by a standard AFM technique [15–19]. However, a nanoring structure has never been reported in these systems. It is highly probable this is due to the drying process that is present in this standard technique; a polyelectrolyte sample is prepared *ex situ* in the AFM apparatus, dried or dehydrated, and then placed in the AFM sample holder for observation. The AFM technique used in this work avoids sample drying and allows nanoring observation.

An important aspect concerning this novel polyelectrolyte nanostructure is therefore the stability. Nanorings produced in MES–TRIS buffer were kept in the liquid cell and followed for a period of 9 h, the AFM images are shown in figure 7. Nanorings are always present and they have grown from 440 ± 52 to 560 ± 75 nm, which represent a variation of the outer diameter average of 27%. Kinetic effects are opposite and of the same order of magnitude to

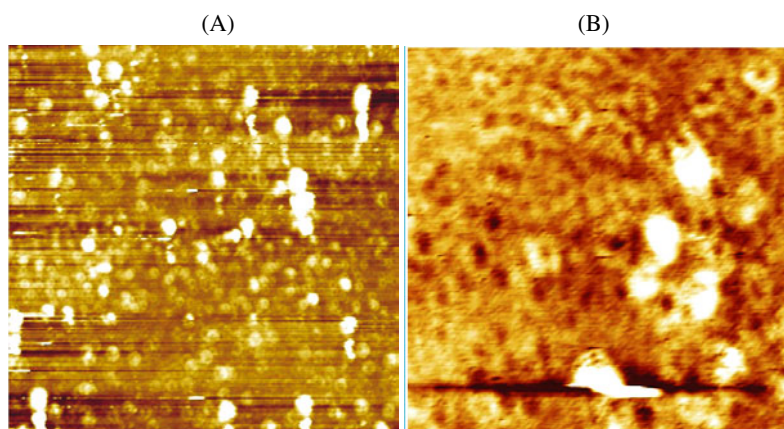


Figure 6. Ring structure is formed using a carbonate buffer. Successful results were obtained at (A) pH = 8.5 and (B) pH = 9.0. The ring structure is less stable than that obtained in a MES–TRIS buffer (images: $10 \times 10 \mu\text{m}$; z range: (A): 30 nm, (B): 15 nm).

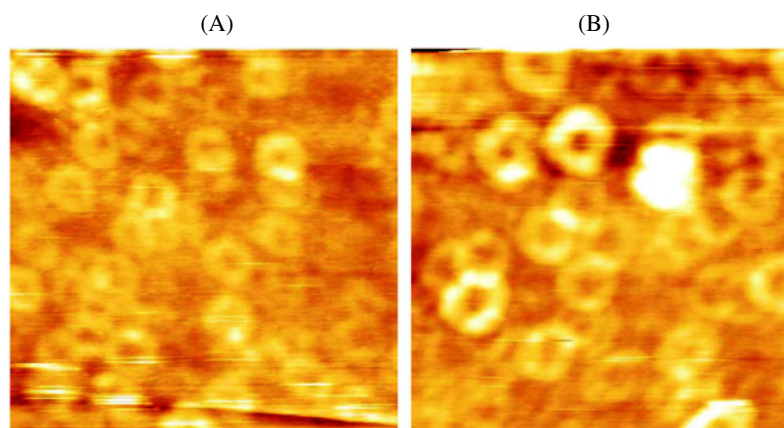


Figure 7. PEI–PSS rings after (A) 1 h and (B) 9 h of PSS injection. Ring dimensions change with time (images: $2.5 \times 2.5 \mu\text{m}$; z range: 8 nm).

those observed for a PSS granulate surface in a thicker film [1], where the grain size is reduced from 133 to 93 nm in 4 h, which represents a variation of 30% in a shorter time.

The stability of the nanorings was also tested when a third positive polyelectrolyte was injected. PAH is injected into the PEI–PSS nanorings and the structure is kept, but ring dimensions change due to the third polyelectrolyte. Nanorings, before and after PAH adsorption, are shown in figures 8(A) and (B), respectively. The dimensions for these figures are D : 304 ± 14 and 352 ± 21 nm; d : 65 ± 8 and 58 ± 14 nm; h : 1.8 ± 0.7 and 2.1 ± 0.6 nm, respectively. We can observe from these values that the ring thickness, defined as $(D - d)/2$, grows an average of 27 nm but that the height is little changed. Therefore, height is practically constant, but the nanorings are thicker. This gives us the possibility of controlling the dimension of the nanorings following the SAPFs build-up.

In contrast with the nanorings produced in MES–TRIS buffer, nanorings obtained in carbonate buffer are less stable at the same experimental conditions. The nanorings shown in

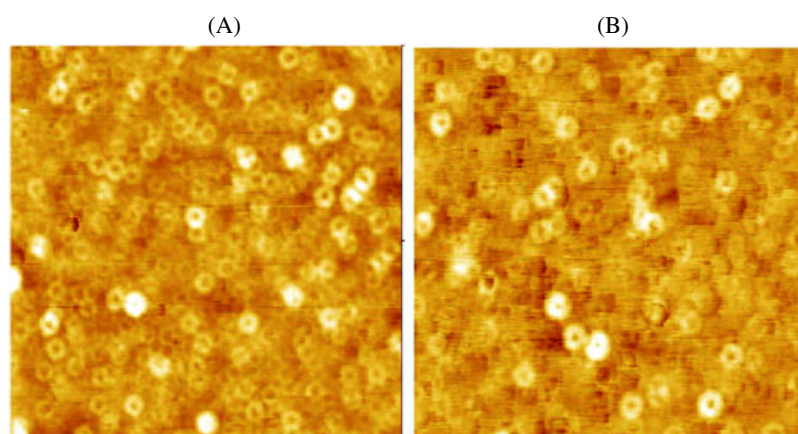


Figure 8. (A) PEI-PSS layer and (B) PEI-PSS-PAH layer. Ring structure formed by PEI-PSS is kept when the PAH polyelectrolyte is injected. However, ring dimensions change due to the third polyelectrolyte (image: $5 \times 5 \mu\text{m}$; z range: 10 nm).

figure 6 are extremely unstable. Those pictures were the only ones obtained for this buffer. Nanorings could not be scanned a second time by the AFM tip.

It is important to say that the most critical parameter in producing nanorings in our experiments was the use of filtered polyelectrolyte solutions. This point is of great importance in this work. Nanorings are only produced when polyelectrolytes are filtered prior to injection into the liquid-cell AFM. Moreover, the nanoring dimensions are directly correlated with filter pore size: a bigger filter pore size produce bigger nanorings. Preliminary results, with all the observed nanorings, give the following correlation: filter pore sizes of 0.10, 0.22 and $0.45 \mu\text{m}$ produce rings with outer diameters of 340 ± 50 , 425 ± 125 and 800 ± 210 nm, respectively. This effect may be related to polyelectrolyte agglomerates produced by filtration. This has been observed for PSS in water by dynamic light scattering (DLS): size of agglomerates are directly correlated with filter pore size [20]. In order to understand this correlation, supplementary DLS and liquid-cell AFM experiments are being realized in our laboratories.

The experimental results presented in this work raise many questions concerning the formation, kinetics and stability of this new structure formed by self-assembling polyelectrolytes. Evidently, further experimental and theoretical work is necessary to understand this nanoring structure. It is particularly interesting to know whether the nanorings reported here have a correspondence with DNA condensation.

4. Conclusions

Self-assembled polyelectrolyte nanorings were observed by liquid-cell AFM. They are obtained with PEI and PSS polyelectrolytes in MES-TRIS and carbonate buffers. Nanorings were observed on a glass surface when PEI and PSS are injected one after the other but also when PEI-PSS complexes are prepared prior to injection, indicating that complexes of positive and negative polyelectrolytes form the nanorings. Nanorings present opposite kinetic effects to granulate film structures reported previously [1]: the size of the nanorings increase with time while grains from granulate structures decrease in size with time. Nanoring sizes range from 300 nm to $2.7 \mu\text{m}$ with a dispersion of 6–18%, depending on the preparation method and parameters such as polyelectrolyte filtration, air and CO_2 exposition and buffer used.

The CO₂ adsorption in water plays an important role because it produces carbonate ions in water, which seem to be mainly responsible for the nanoring formation. Carbonate buffers at high pH values were used to control divalent carbonate ions and nanorings were successfully observed. However, the nanorings are less stable than those obtained in MES–TRIS buffers.

These structures have only been observed in the liquid-cell of the AFM. They are destroyed during the drying process that occurs in standard AFM experiments. An additional and important condition for observing nanorings is the utilization of filtered polyelectrolyte solutions.

Mechanisms that produce nanorings at the beginning of SAPFs formation are an open question. They are probably close to those that produce DNA condensation. The internal structure of the PEI–PSS complex may also play an important role in the formation of these nanorings, as recognized in the formation of other nanostructures. Further theoretical and experimental work is necessary to understand this novel structure. Future applications can also be envisaged, for example: fabrication of nano-membranes and surfaces with specific sites to adsorb particles and metals.

Acknowledgments

This work was partially supported by the ‘Biomolecular Materials Project’: CONACYT-Mexico (ER026), Mexico–France programme: SEP-CONACYT-ANUIES-ECOS France (M01-S01) and PROMEP (UASLP-F-4). JLM and HF thank CONACYT and PROMEP for their PhD scholarships, respectively.

References

- [1] Menchaca J-L, Jachimska B, Cuisinier F and Pérez E 2003 *Colloids Surf. A* **222** 185
- [2] Decher G 1997 *Science* **277** 1232
- [3] Messina R 2004 *Macromolecules* **37** 621
- [4] Castelnuovo M and Joanny J F 2000 *Langmuir* **16** 7524
- [5] Park S Y, Rubner M F and Mayes A M 2002 *Langmuir* **18** 9600
- [6] Taylor W H and Hagerman P J 1990 *J. Mol. Biol.* **212** 363
- [7] Bloomfield V A 1996 *Curr. Opin. Struct. Biol.* **6** 334
- [8] Gelbart W M, Bruinsma R F, Pincus P A and Parsegian V A 2000 *Physics Today* **53** 38
- [9] Manning G S 1969 *J. Chem. Phys.* **51** 924
- [10] Lozada-Cassou M and Jiménez-Angeles F 2001 *Preprint physics/0105043 v2*
- [11] Shen M S, Downing K H, Balhorn R and Hud N V 2000 *J. Am. Chem. Soc.* **122** 4833
- [12] Hartgerink J D, Granja J R, Milligan R A and Ghadri M R 1996 *J. Am. Chem. Soc.* **118** 43
- [13] Okamoto H, Nakanishi T, Nagai Y, Kasahara M and Takeda K 2003 *J. Am. Chem. Soc.* **125** 2756
- [14] Drever J I 1997 *The Geochemistry of Natural Water: Surface and Groundwater Environments* (Englewood Cliffs, NJ: Prentice-Hall)
- [15] Mendelsohn J D, Barrett C J, Chan V V, Pal A J, Mayes A M and Rubner M F 2000 *Langmuir* **16** 5017
- [16] McAloney R A, Sinyour M, Dudnik V and Goh M C 2001 *Langmuir* **17** 6655
- [17] Tsukruk V V, Bliznyuk V N, Visser D, Campbell A L, Bunning T J and Adams W W 1997 *Macromolecules* **30** 6615
- [18] Lobo R F M, Pereira-da-Silva M A, Raposo M, Faria R M and Oliveira O N 1999 *Nanotechnology* **10** 389
- [19] Lavalle Ph, Gergely C, Cuisinier F J G, Decher G, Schaaf P, Voegel J-C and Picart C 2002 *Macromolecules* **35** 4458
- [20] Sedlak M 2002 *J. Chem. Phys.* **116** 5236
- [21] Cohen Stuart M A, Besseling N A M and Fokink R G 1998 *Langmuir* **14** 6846